Title: Genomic footprints of local adaptation along elevation gradients associate with present phenotypic variation in teosintes

Short Title: Linking selective footprints to phenotypes in teosintes

M-A. Fustier[1,☯], N.E. Martínez-Ainsworth[1,☯], A. Venon[1], H. Corti[1], A. Rousselet[1], F. Dumas[1], H. Dittberner[2], J.A. Aguirre-Liguori[3], M.G. Camarena[4], D. Grimanelli[5], M. Falque[1], L. Moreau[1], J. de Meaux[2], S. Montes-Hernandez[4], L.E. Eguiarte[3], Y. Vigouroux[5], D. Manicacci[1,*], M.I. Tenaillon[1,*]

[1] : Génétique Quantitative et Evolution – Le Moulon, Institut National de la Recherche Agronomique, Université Paris-Sud, Centre National de la Recherche Scientifique, AgroParisTech, Université Paris-Saclay, France

[2]: Institute of Botany, University of Cologne Biocenter, 47b Cologne, Germany

[3]: Departamento de Ecología Evolutiva, Instituto de Ecología, Universidad Nacional Autónoma de México, Ciudad de México, Mexico

[4] : Campo Experimental Bajío, Instituto Nacional de Investigaciones Forestales, Agrícolas y Pecuarias, Celaya, Mexico

[5] : Université de Montpellier, Institut de Recherche pour le développement, UMR Diversité, Adaptation et Développement des plantes, Montpellier, France

☯: The authors equally contributed to this work

* co-corresponding authors

E-mail: domenica.manicacci@inra.fr, maud.tenaillon@inra.fr

Abstract

Local adaptation across species range is widespread. Yet, much has to be discovered on its environmental drivers, the underlying functional traits and their molecular determinants. Because elevation gradients display continuous environmental changes at a short geographical scale, they provide an exceptional opportunity to investigate these questions. Here, we used two common gardens to phenotype 1664 plants from 11 populations of annual teosintes. These populations were sampled across two elevation gradients in Mexico. Our results point to a syndrome of adaptation to altitude with the production of offspring that flowered earlier, produced less tillers, and larger, longer and heavier grains with increasing elevation. We genotyped these plants for 178 outlier single nucleotide polymorphisms (SNPs), which had been chosen because they displayed excess of allele differentiation and/or correlation with environmental variables in six populations with contrasted altitudes. A high proportion of outlier SNPs associated with the phenotypic variation of at least one trait. We tested phenotypic pairwise correlations between traits, and found that the higher the correlation, the greater the number of common associated SNPs. In addition, allele frequencies at 87 of the outlier SNPs correlated with an environmental component best summarized by altitudinal variation on a broad sample of 28 populations. Chromosomal inversions were enriched for both phenotypically-associated and environmentally-correlated SNPs. Altogether, our results are consistent with the set-up of an altitudinal syndrome promoted by local adaptation of teosinte populations in the face of gene flow. We showed that pleiotropy is pervasive and potentially has constrained the evolution of traits. Finally, we recovered variants underlying phenotypic variation at adaptive traits. Because elevation

mimics climate change through space, these variants may be relevant for future maize breeding.

Keywords: spatially-varying selection; F_{st}-scan; association mapping; altitudinal syndrome; pleiotropy; chromosomal inversions;

Author summary

Across their native range, species encounter a diversity of habitats promoting local adaptation of geographically distributed populations. While local adaptation is widespread, much has yet to be discovered about the conditions of its emergence, the targeted traits, their molecular determinants and the underlying ecological drivers. Here we employed a reverse ecology approach, combining phenotypes and genotypes, to mine the determinants of local adaptation of teosinte populations distributed along two steep altitudinal gradients in Mexico. Evaluation of 11 populations in two common gardens located at mid-elevation pointed to the set-up of an altitudinal syndrome, in spite of gene flow. We scanned genomes to identify loci with allele frequencies shifts along elevation. Interestingly, variation at these loci was commonly associated to variation of phenotypes. Because elevation mimics climate change through space, these variants may be relevant for future maize breeding.

Introduction

Local adaptation is key for the preservation of ecologically useful genetic variation [1]. The conditions for its emergence and maintenance have been the focus of a long-standing debate nourished by ample theoretical work [2–9]. On one hand, spatially-varying selection promotes the evolution of local adaptation, provided that there is genetic diversity underlying the variance of fitness-related traits [10]. On the other hand, opposing forces such as neutral genetic drift, temporal fluctuations of natural selection, recurrent introduction of maladaptive alleles via migration among populations and homogenizing gene flow may hamper local adaptation (reviewed in [11]). Empirical evidence for local adaptation is brought by measures of reciprocal native-site fitness advantage [11]. Meta-analyzes indicate that local adaptation is pervasive, with evidence through reciprocal transplants detected in 45% to 71% of populations [12,13].

While local adaptation is widespread, much has yet to be discovered about the traits submitted to spatially-varying selection, their molecular determinants and the underlying ecological drivers [14]. Empirical studies on these important questions rely on the predictions that local adaptation increases with phenotypic, genotypic and environmental divergence among populations [2,15,16]. Comparisons of the quantitative genetic divergence of a trait (Q_{st}) with the neutral genetic differentiation (F_{st}) can provide hints on whether trait divergence is driven by spatially-divergent selection [17–20]. Application of these approaches reveals striking examples of divergent selection for developmental rate in the common toad [21], for drought and frost tolerance in alpine populations of the European silver fir [22], and for traits related to plant phenology, size and floral display among populations of *Helianthus* species [23,24].

At the genomic level, local adaptation is usually detected by genomic regions harboring population-specific signatures of selection. These signatures include alleles displaying greater-than-expected differentiation among populations [25] and can be identified through F_{st}-scans [26–32]. F_{st}-scans and its derivative methods [26–32], however, suffer from a number of limitations, among them the high number of false positives (reviewed in [33,34]) and the lack of power to detect true positives [35]. Despite these caveats, F_{st}-outlier approach has brought emblematic allele discoveries such as at *EPAS1*, a gene involved in the adaptation to altitude in Tibetan human populations [36]. An alternative to detect locally adaptive loci is to test genotype-environment correlation [32,37–42]. Correlation-based methods have proven to be more powerful than differentiation-based methods [43]. However, spatial autocorrelation of population structure and environmental variables can lead to spurious signatures of selection [44].

Both differentiation and environmental genome scans recover sets of outlier loci, a proportion of which are false positives [45]. Ultimately, a link between outliers and phenotypic variation therefore needs to be established. Replicated common gardens of *Arabidopsis* ecotypes have shown that fitness-associated alleles display geographic and climatic patterns of selection [46]. Another study, demonstrated that the relative fitness of *Arabidopsis* accessions in a given environment could actually be predicted from climate-associated SNPs [47]. While it is clear that climatic selection over broad latitudinal scales produces genomic and phenotypic patterns of local adaptation in the selfer plant *Arabidopsis*, whether such patterns would persist in the face of gene flow, at shorter spatial scale and/or in outcrossing species remains to be elucidated. More importantly, the question of whether loci exhibiting footprints of selection are relevant for present day phenotypic variation in natural populations remains open.

We focused on a well-established outcrossing plant system, the teosintes, to investigate the relationship of molecular, environmental, and fitness variation in populations sampled across two elevation (climatic) gradients in Mexico. Teosintes are the closest wild relatives of maize and encompass two annual subspecies, *Zea mays* ssp. *parviglumis* (hereon *parviglumis*) and *Zea mays* ssp. *mexicana* (hereon *mexicana*). Both display large effective population sizes [48], and span a diversity of climatic conditions, from warm and mesic conditions below 1800 m for *parviglumis*, to drier and cooler conditions up to 3000 m for *mexicana* [49]. Previous studies have discovered potential determinants of local adaptation in these systems. At a genome-wide scale, decrease in genome size correlates with increasing altitude, which likely results from the action of natural selection on life cycle duration [50, 51]. More modest structural changes include megabase inversions that harbor clusters of SNPs whose frequencies are associated with environmental variation [52, 53]. Also, differentiation- and correlation-based genome scans in six teosinte populations succeeded in finding outlier SNPs for local adaptation [54, 55].Yet, a link with phenotypic variation has yet to be established.

In this paper, we used teosinte populations distributed along two altitudinal gradients covering a relatively short yet climatically diverse, spatial scale. Both gradients encompass populations from the two subspecies that are the closest wild relatives of maize, *Zea mays* ssp. *parviglumis* and *Z. mays* ssp. *mexicana*. We first performed common garden experiments on a subset of 11 populations, for which we evaluated 18 phenotypic traits in two locations over two consecutive years. We genotyped individuals from this association panel at outlier SNPs detected from whole genome sequencing of six populations, as well as at 38 microsatellite markers. We next genotyped outlier and neutral SNPs on an extended sample of 28 teosinte populations. We address three main questions: Is there a suite of traits that

defines a syndrome of adaptation to altitude in teosintes? How powerful are genome scans to detect variants involved in present phenotypic variation? What are the genetic and environmental drivers of its evolution?

Results

Phenotypic variation within and among populations.

In order to investigate phenotypic variation, we set up two common garden experiments located at mid-elevation in Mexico to evaluate individuals from 11 teosinte populations (S1 Fig, S1 Table). These populations were sampled among 37 populations distributed along two altitudinal gradients from lowland populations of the subspecies *parviglumis* (8) to highland populations of the subspecies *mexicana* (3) (S2 Fig). They were therefore climatically contrasted as can be appreciated in the Principal Component Analysis (PCA) computed on 19 environmental variables (S3 Fig). The corresponding set of individuals from the 11 populations formed our association panel.

We gathered phenotypic data during two consecutive years (2013 and 2014). We targeted 18 phenotypic traits that included six traits related to plant architecture, three traits related to leaves, three traits related to reproduction, five traits related to grains, and one trait related to stomata (S2 Table). Each of the four experimental assays (year-field combinations) encompassed four blocks. In each block, we evaluated one offspring of ~15 mother plants (half-sibs) from each of the 11 teosinte populations using a semi-randomized design. After filtering for missing data, our association panel encompassed 1664 teosinte individuals.

We found significant effects of Field, Year and/or their interaction for most traits (model M1, S3 Table), and a highly significant effect of the population for all of them (S3 Table). Principal component analysis including all phenotypic measurements highlighted the distinction between *parviglumis* and *mexicana* subspecies along PC1 (Fig 1A), an axis that strongly correlated with altitude (Fig 1B & 1C). Furthermore, while populations of each subspecies largely overlapped, we observed a consistent tendency within subspecies for population phenotypic differentiation along PC1, irrespective of the gradient (Fig 1C). Traits that correlated the most to PC1 were grain-related traits, tillering, and female and male flowering time (Fig 1B). PC2 instead correlated with traits exhibiting a trend toward increase-with-elevation within *parviglumis*, but decrease-with-elevation within *mexicana* (Fig 1D). PC2 correlated with vegetative growth-related traits such as plant height, height of the lowest and highest ear (Fig 1B). Together, both axes explained 37% of the phenotypic variation.

We investigated in greater detail the influence of altitude on each trait independently. All traits, except for the number of nodes with ears (NoE), exhibited a significant effect of altitude (S3 Table, M3 model). Note that after accounting for elevation, the population effect remained significant for all traits (data not shown), suggesting that other factors than altitude also contributed to shape phenotypic variation among populations. Traits related to flowering time and tillering displayed a continuous decrease with elevation, and traits related to grain size increased with elevation (Fig 2 & S4 Fig). Stomata density also diminished with altitude (Fig 2). In contrast, traits related to PC2 (e.g., plant height, height of the lowest ear, height of the highest ear, Fig 1B&1D) displayed maximum values at intermediate altitudes (highland *parviglumis* and lowland *mexicana*) (S4 Fig). We estimated narrow-sense heritabilites (additive genotypic effect) per population for all traits using a mixed ‘animal’ model. Average heritabilities per trait ranged from 0.154 for leaf color to 0.644 for female flowering

time (S2 Table). We obtained higher heritabilities for grain related traits when mother plant measurements were included in the model with 0.631 (*SD* = 0.246), 0.511 (*SD* = 0.043) and 0.274 (*SD* = 0.160) for grain length, weight and width, respectively, as compared to when they were not included.

Altogether, the continuous variation of a subset of traits across populations in both elevation gradients was consistent with a syndrome where populations produced less tillers, flowered earlier and carried larger, longer and heavier grains with increasing elevation (S4 Fig).

Figure 1: Principal Component Analysis on phenotypic values corrected for the experimental setting. Individuals factor map (A) and corresponding correlation circle (B) on the first two principal components with altitude added as a supplementary variable (in blue). Individual phenotypic values on PC1 (C) and PC2 (D) are plotted with populations ranked by altitude and color-coded following A. For populations from the two subspecies, *parviglumis* (circles) and *mexicana* (triangles), color intensity indicates ascending elevation in green for *parviglumis* and red for *mexicana*. Corrections for experimental setting are detailed in Model M2.

Figure 2: Box-plots of adjusted means for four traits. Traits are female flowering time (A), male flowering time (B), grain length (C) and stomata density (D). Populations are ranked by altitude. *Parviglumis* populations are shown in green and *mexicana* in red, lighter colors are used for gradient ‘a’ and darker colors for gradient ‘b’. Units of measurement are detailed in S2 Table. In the case of flowering times, we report data for 9 out of 11 populations because most individuals from the two lowland populations (P1a and P1b) did not flower in

our common gardens. Covariation with elevation was significant for the four traits. Corrections for experimental setting are detailed in Model M'1.

Identification of traits under spatially-varying selection.

To identify traits whose variation among populations was driven primarily by local selection, we contrasted genetic differentiation (F_{st}) and phenotypic differentiation (Q_{st}). We computed F_{st} using 38 SSRs (S4 Table). This analysis encompassed a total of 1125 plants of our association panel, for which we had both individual phenotypes and individual genotypes.

Q_{st} was significantly larger than F_{st} for eight traits: grain length, width and weight, number of tillers, heights of the highest and lowest ears, female and male flowering time (Fig 3). Among these traits, six were among the most correlated with altitude (Fig 1B) and exhibited a marked altitudinal pattern of variation: grain length, width and weight, number of tillers, and female and male flowering time (Fig. 2, S4 Fig).

Figure 3: Significance of Q_{st}-F_{st} difference for each trait. The dotted blue line indicates the 95% threshold of the simulated distributions and the red line refers to the observed difference. We considered as spatially-varying traits those for which the observed difference fell outside the 95% threshold.

Structuring of adaptive and neutral genetic diversity.

We successfully genotyped 218 (~81%) out of the 270 outlier SNPs, of which 141 were previously detected in candidate regions for local adaptation [55]. Candidate regions were identified from re-sequencing data of six teosintes populations (S1 Table) following an approach that included high differentiation between highlands and lowlands, environmental

correlation, and in some cases their intersection with genomic regions involved in quantitative trait variation in maize. The remaining ones (77) were discovered in the present study by performing F_{st}-scans on the same re-sequencing data (S1 Table, S5 Table). We detected outlier SNPs that were both highly differentiated between the two pairs of highland and lowland populations (gradients *a* and *b*), while still segregating and displaying a pattern of differentiation by altitude within at least one of the two subspecies. F_{st}-scans pinpointed three genomic regions of particularly high differentiation (S5 Fig) that corresponded to previously described inversions [52,53]: one inversion on chromosome 1 (*Inv1n*), one on chromosome 4 (*Inv4m*) and one on the far end of chromosome 9 (*Inv9e*). The 218 outlier SNPs were distributed along the 10 chromosomes of maize, and exhibited low level of linkage disequilibrium (LD), except for SNPs located on chromosomes eight, nine, and a cluster of SNPs located on chromosome 4 (S6 Fig).

We compared the neutral genetic structure of the association panel revealed by SSRs to the genetic structure revealed by outlier SNPs. For SSRs, the highest likelihood was obtained at K = 2 and K = 5 clusters. At K=2, we found a clustering associated with subspecies differentiation between *mexicana* and *parviglumis* (data not shown). At K=5, we observed an additional layer of structuration associated to both altitudes and gradients (Fig 4A & 4B). In contrast, the genetic structure recovered from the 218 outlier SNPs formed three clusters (K=3) (Fig 4C). As expected, their geographical distribution revealed a structuring by altitude irrespective of the gradient (Fig 4D). Noteworthy was the lowland group that encompassed geographically distant populations from the two gradients (Fig 4D).

Figure 4: Comparison of genetic clustering revealed by 38 neutral SSRs and 178 outlier SNPs. The comparison was established on a subset of 1,426 individuals from our association

panel, for which both SSR and SNP genotyping was available. For SSRs and outlier SNPs, the marginal likelihood was maximized at K=5 (A) and K=3 (C), respectively. Colors represent the K clusters. Individuals (vertical lines) are partitioned into colored segments whose length represents the membership proportions to the K clusters. Populations (names after subspecies names M: *mexicana*, P: *parviglumis* and gradient 'a' or 'b') are ranked by altitude indicated in meters. The corresponding geographic distribution of populations along with their average membership probabilities are plotted for SSRs (B) and outlier SNPs (D).

Associating genotypic variation at outlier SNPs to phenotypic variation.

We tested the association between phenotypes and 178 outlier SNPs (MAF>5%) using our association panel. For each SNP-trait combination, the sample size ranged from 264 to 1068, with a median of 1004 individuals (S6 Table). We used neutral SSRs to correct for both structure and kinship. This model resulted in a uniform distribution of P-values when testing the association between genotypic variation at SSRs and phenotypic variation at traits (S7 Fig). Under this model, we found that 148 outlier SNPs (83.1%) associated to at least one trait (Fig 5 and S8 Fig) at an FDR of 5%.

A growing body of literature stresses that incomplete control of population stratification may lead to spurious associations [56]. Hence, highly differentiated traits along environmental gradients are expected to co-vary with any variant whose allele frequency is differentiated along the same gradients, without underlying causal link. We actually found a borderline significant correlation (P-value=0.03) between the strength of the population effect for each trait – a measure of trait differentiation (S3 Table) – and its number of associated SNPs (S5 Table). The correlation however disappeared after removing male and female flowering time. The level of differentiation between the two subspecies in our outcrossing

system was relatively low (F_{st} ≈12%, 55). As a comparison, in the selfer *Arabidopsis thaliana*, differentiation among populations from the same geographical area varies between 29% and 80% [57]. Subspecies differentiation was fully accounted for in SSRs genetic structuring as shown by the clear distinction between *mexicana* populations and the rest of the samples (Fig 4A). To verify that additional layers of structuring among populations did not cause an excess of spurious associations, we randomized phenotypes within populations, positing that if associations indeed originated from under-correction of population structure, they would persist after randomization. We performed this analysis for female flowering time. We observed an average of 0.06 significant SNP associations for female flowering time over 50 randomizations, instead of 59 originally detected. This striking difference suggests that the majority of our associated SNPs are true positives.

The number of associated SNPs per trait varied from three SNPs for leaf length as for stomata density, to 61 SNPs for male flowering time, with an average of 26.7 SNPs per trait (S5 Table). About half (54.6%) of associated SNPs were common to at least two traits (S5 Table), and the remaining 49 SNPs were associated to a single trait (S5 Table). The group of eight traits displaying evidence of spatially varying selection in the Q_{st}-F_{st} analyses displayed a greater number of SNPs associated per trait (36.4 on average), compared to the non-spatially varying traits (19.1 on average). Finally, one striking feature of our results was that inversions of chromosomes 1, 4, and 9, taken together, were enriched for associated SNPs associated with phenotypes (χ^2 = 5.11, P-value=0.02).

Figure 5: Manhattan plots of associations between 178 outlier SNPs and four phenotypic traits. X-axis indicates the positions of outlier SNPs on chromosomes 1 to 10,

black and gray colors alternating per chromosome. The red lines indicate significance thresholds at 5% FDR, with associated SNPs above those lines colored accordingly.

Drivers of correlation between traits.

Traits related to development, phenology and fitness are not independent. In order to evaluate their correlations, we computed pairwise-correlations between traits after correcting for experimental design and population structure (K=5) for all traits. We found 63 (41%) significant correlations among 153 tested pairs of traits. Among the strongest positive correlations, were the following pairs of traits: male and female flowering time, plant height and height of the highest ear, height of the highest and lowest ear, grain length and width (Fig 6A). The correlation between female (or male) flowering time with grain weight was among the strongest negative correlations (Fig 6A).

We next asked whether the strength of the pairwise correlations between traits depended on the number of common associated SNPs, i.e. SNPs associated significantly with the variation of the two traits considered in the pairwise correlation. We found a significant and positive correlation (Fig 6B). This correlation persisted even after removing the strongest correlation between male and female flowering time. To summarize, our results showed a large proportion of significantly correlated traits, and the traits that were the most correlated also displayed significantly more common associated SNPs.

Figure 6: Pairwise correlations between phenotypic traits, and number of common associated SNPs. The matrix of phenotypic pairwise correlations (Pearson coefficient sign and magnitude for significant correlations) is shown along with the number of common associated SNPs in black for significant correlations and gray otherwise (A). The correlation

between the absolute value of the pairwise phenotypic correlation coefficient and the excess of common associated SNPs (B) is significant (Pearson r=0.41, P-value=4.16 10^{-6}; Kendall r=0.19, P-value=1.8 10^{-3}; regression line is indicated in red). It remained significant after discarding the most outlier data point (the pairwise correlation between female and male flowering time >0.8). Black and gray dots refer to significant and not significant pairwise correlations respectively.

We considered the four year-field assays as different experimental environments. We used the blocks within them as replicates to explore the consistency of pairwise phenotypic correlations across experimental environments and populations (4x4=16 correlation values). We formulated the following interpretations: (1) correlations consistent across both experimental environments and populations most likely reflects genetic mechanisms constraining the independent evolution of traits; (2) correlations consistent across experimental environments within one or few populations may be best explained by population-specific adaptive correlation; (3) plastic response in our common garden setting would generate environmental-specific correlations regardless of the population.

Among 63 significant pairwise correlations that had common associated SNPs, 96.8% exhibited neither treatment nor population effects, and therefore likely resulted from underlying genetic constraints (S9 Fig). This was the case for male and female flowering time, for height of the lowest and highest ear, grain length and width, for instance. Only six correlations displayed population effects such as male flowering time and leaf length for instance (S9 Fig). However, close inspection of the results revealed that population effect was always driven by one or two extreme populations with a paucity of data (data not shown). Finally, we found eight correlations with a significant experimental environment effect which

may reflect a plastic response common to all populations (S9 Fig). The correlation between plant height and height of the highest ear fell in that category. Note that two pairwise correlations (plant height with grain length, and height of the highest ear and grain length) displayed a pattern consistent with a population-specific plastic response (experimental environment x population interaction effect).

Environmental variables underlying local adaptation.

In order to analyze the environmental patterns correlating to our 218 outlier SNPs frequencies, we genotyped an extended sample of 28 populations distributed along the two elevation gradients. We assessed correlation between outlier SNPs and 19 climatic variables. Because climatic variables are not independent, we summarized environmental information from the sampled populations by two principal components (PCenv1 and PCenv2). The first component that explained 56% of the variation correlated with altitude, and was defined both by temperature- and precipitation- related variables (S3 Fig) such as the Minimum Temperature of Coldest Month (T6), Mean Temperature of Driest and Coldest Quarter (T9, T11), Precipitation of Driest Month and Quarter (P14, P17). The second PC explained 20.5% of the variation and was mainly defined (S3 Fig) by Isothermality (T3), Temperature Seasonality (T4) and Temperature Annual Range (T7).

Roughly 53% (115) of the 218 outlier SNPs associated with at least one of the two first PCenvs, with 98 and 33 associated with PCenv1 and PCenv2, respectively. Among those that were tested for phenotypic association (178), we found 104 (58%) that were associated to the first two environmental components, either exclusively to PCenv1 (71) or PCenv2 (17), or both (16) (S10 Fig, S1 Fig).

SNPs correlating with PCenvs were not more often associated to phenotypes than expected by chance ($\chi^2 = 0.13\ 10^{-5}$, P-value=0.99). Inversions, however, were enriched for SNPs correlating with PCenv1 ($\chi^2 = 18.55$, P-value=$1.66\ 10^{-5}$). Finally, SNPs associated to spatially varying traits associated more often than expected to environmental PCenv1 ($\chi^2 = 7.85$, P-value = $5\ 10^{-3}$), but not to PCenv2 ($\chi^2 = 2.19$, P-value= 0.14).

Discussion

Local adaptation of plant populations sampled across vast geographical ranges has been well documented. Population genomics has brought a flurry of tools to detect outlier loci with footprints of local adaptation across populations, but the multiplicity of confounding factors has questioned their reliability for detecting outlier loci underlying adaptive processes. As a result, whether loci exhibiting footprints of selection are relevant for present day phenotypic variation in natural populations is an open question. Ultimately, it is the intertwining of trait, molecular, and environmental variation that is paramount for the study of local adaptation.

Here we investigated those links on a well-established outcrossing system, the closest wild relatives of maize, along altitudinal gradients that display considerable environmental shifts over short geographical scales. We used populations that range from 504 to 2176 m in altitude over ~460 kms for gradient *a*, and from 342 to 2581m in altitude over ~350 kms for gradient *b* (S2 Fig). We genotyped 28 populations at 218 outlier SNPs detected with population genomic tools, and determined population values for 19 climatic variables (S1 Table). In parallel, we conducted an association analysis using individuals derived from

grains collected from 11 of those populations. We phenotyped individuals in two common gardens for two years, and genotyped them at neutral markers and outlier SNPs.

Syndrome of adaptation to altitude.

Common garden studies of adaptation along elevation gradients have been conducted in European and North American plants species [58]. Together with other studies, they have revealed that adaptive responses to altitude are multifarious [59]. They include physiological responses such as high photosynthetic rates [60], tolerance to frost [61], biosynthesis of UV-induced phenolic components [62]; morphological responses with reduced stature [63,64], modification of leaf surface [65], increase in leaf non-glandular trichomes [66], modification of stomata density; and phenological responses with variation in flowering time [67], and reduced growth period [68].

Our multivariate analysis on phenotypes revealed a marked differentiation between subspecies along the first axis (21.26% of the total variation) that also discriminated populations by altitude (Fig 1B). Because convergence of phenotypes may be caused by shared population history, we controlled for neutral genetic differentiation. We identified six traits that exhibited a pattern consistent with both spatially-varying selection (Fig 3) and a clinal increase/decrease of population average phenotypic differences with elevation (S4 Fig). These traits collectively defined a teosinte altitudinal syndrome of adaptation characterized by early-flowering, production of few tillers and of heavy, long and large grains. We also observed increased leaf pigmentation with elevation, although with a less significant signal (S3 Table), consistent with the pronounced difference in sheath color reported between *parviglumis* and *mexicana* [69,70].

We recovered a trend towards depleted stomata density at high altitudes (S4 Fig). This trend could arguably represent a physiological adaptation as stomata influence components of plant fitness through their control of transpiration and photosynthetic rate [71]. Indeed, in natural accessions of *A. thaliana*, stomatal traits showed signatures of local adaptation and were associated with both climatic conditions and water-use efficiency [72]. Furthermore, previous work has shown that in arid and hot highland environments, densely-packed stomata may promote increased leaf cooling in response to desiccation [73] and may also counteract limited photosynthetic rate with decreasing pCO_2 [74]. Accordingly, increased stomata density with elevation has been reported in Alpine species such as the European Beech [75]. In our case, higher elevations display arid but *cooler* temperatures during the growing season, features perhaps more comparable to other tropical mountains for which a diversity of patterns in stomatal density variation with altitude has been reported [76]. Further work will be needed to decipher the mechanisms driving the pattern of declining stomata density with altitude in teosintes.

Several elements suggest that our observed clinal trends in phenology and morphology reflect genetic differentiation rather than environmental maternal effects. First, if phenotypic traits were strongly influenced by environmental maternal effects, we would not have found strong associations with genetic polymorphisms (Fig 5, S8 Fig). For grain lenght and weight, we more finely ruled out a strong mother plant effect since we estimated high heritabilites ($h^2 > 0.5$). Second, a greenhouse experiment reported similar trends for 17 accessions of annual teosintes including both *parviglumis* and *mexicana* [77]. Consistently with our findings, the aforementioned study revealed reduced tiller number, as well as increase in grain weight and grain number per ear and increase in leaf width with altitude [77].

Altogether, the altitudinal syndrome was consistent with natural selection for rapid life-cycle shift, with early-flowering in the shorter growing season of the highlands and production of larger propagules than in the lowlands. Although we did not formally measure biomass production, the lower number of tillers and higher amount and size of grains in the highlands as compared with the lowlands may reflect trade-offs between allocation to grain production and vegetative growth [78]. Because grains fell at maturity and a single teosinte individual produces hundreds of ears, we were unable to provide a proxy for total grain production. The existence of fitness-related trade-offs therefore still needs to be formally addressed.

Beyond trade-offs, our results more generally question the extent of correlations between traits, and the part of the phenotypic responses that are due to such correlations rather than local adaptation. In maize, for instance, we know that female and male flowering time are positively correlated [79], and themselves correlate with yield-related traits [80]. Response to selection for late-flowering also triggers a correlated increase in leaf number in cultivated maize [81], and common genetic loci have been shown to determine both traits [82]. Whether such correlations result from modern breeding or exist in teosintes remains to be established. We took advantage of our phenotypic measures to evaluate pairwise correlations between traits. We found strong positive correlations between male and female flowering time, grain length and width, plant height and height of the lowest or highest ear. Strong negative correlations concerned grain weight with both male and female flowering time. Together these correlations were consistent with observations in maize, most of which resulted from genetic constraints, either due to pleiotropy or linked loci. Such constraints seem therefore to have been inherited from wild ancestors to maize.

Footprints of past adaptation are relevant to detect variants involved in present phenotypic variation.

One of the most striking results of our study is that a large majority of our outlier SNPs (83% at 5% FDR) were associated with phenotypic variation. Given our FDR threshold and except for four traits (leaf length, leaf and grain coloration, stomata density), the number of associated SNPs by far exceeded the number of false positives expected. This result suggests that despite abundant criticisms [35], differentiation- and correlation-based methods are powerful to detect loci associated with adaptive phenotypic variation. It is intriguing in several respects. First, for most outlier SNPs, detection was performed on a subset of only six nonetheless highly differentiated populations. Second, the method used to pinpoint outlier SNPs (basic F_{st} scans *versus* other methods, S5 Table) did not affect the rate by which SNPs associated with phenotypes ($\chi^2_{(df=1)} = 7.97\ 10^{-30}$, P-value ≈ 1.00). Third, while most methods used to detect outlier SNPs were based on allele differentiation *between* populations, there was still enough variation *within* populations to detect genotype-phenotype association signals. This seems to indicate that variation persisted over long time scales despite continuous selection.

The number of SNPs associated per trait varied from 3 to 61, with no association for leaf and grain coloration (S5 Table). Our results therefore point to a high proportion of associated SNPs, and since LD is very limited in teosinte populations (decaying within <100bp, [55]) this indicates that phenotypic variation is driven by numerous independent loci. Consistently, Weber et al. [83] found that individual SNPs account for small proportions of the phenotypic variance. In sum, our results argue in favor of a scenario of polygenic

adaptation where, within population, concerted changes of allele frequencies at many loci collectively contribute to determine phenotypic variation [84].

Another key observation was that a majority of associated SNPs were shared by two or more traits, and the stronger the correlation between traits, the more they displayed common associated SNPs (Fig 6B). Hence, phenotypic correlations are at least partially determined by common genetic variants, suggesting that pleiotropy is pervasive. This is consistent with previous reports showing, for example, that the genetic control of female and male flowering time involves a common set of genes [79]. Note that, while we did not test for epistasis – the effect of marker combinations as opposed to single marker analysis – genome-wide association mapping studies (GWAS) in maize all concur to phenotypic variation being dominated by additive effects [79,85]. Overall, most traits that we studied are highly pleiotropic and have likely evolved under long-term stabilizing polygenic selection [49]. In such context, differences in detection power of our GWAS among traits may reflect differences of trait genetic architecture, that is differences in the number, frequency and effect of variants contributing to heritable variation. For instance, just like in previous studies [79], we detected many SNPs associated with flowering time, but found only three SNPs associated with leaf length and stomata density. It is possible that selection at these latter traits has been less stable over time and/or weaker generating a skew towards low frequency, small effect variants that we were unable to detect [86].

The proportion of genic SNPs associated to phenotypic variation (85%) was not significantly higher than that of non-genic SNPs (78%) (>1kb from a gene) ($\chi^2_{(df=1)} = 0.93$, P-value = 0.334) stressing the importance of considering both types of variants [87]. Several genes that we recovered from our SNPs deserve specific attention (S5 Table). For example, *Eukaryotic Initiation Factor* (*EiF4A*) has been previously pinpointed in maize GWAS for

multiple traits, such as female and male flowering time, plant height [81] and photoperiod response [88]. We also recovered *Sugary1* (*Su1*), a starch debranching enzyme that was selected during domestication and subsequent breeding [89,90]. We found that *Su1* was associated with variation at three traits (flowering time, tillering and tassel branching) pointing to high pleiotropy. A previous study reported association of this gene to oil content in teosintes [83]. We identified association with a SNP at *Sh2* and five traits. Paralogs of *Sh2* expressed in different tissues encode the large subunit of a rate-limiting starch biosynthetic enzyme, and some of them were selected during domestication and breeding [91]. Significant associations with the number of grains per ear and grain weight in teosintes are consistent with the findings that the insertion of a *shrunken-2* (*Sh2*) modified gene in maize can provoke a temperature-dependent increase in grain number [92].

Environmental variables driving local adaptation.

A substantial proportion of our set of outlier SNPs was chosen due to their significant correlation among six populations between variation of allele frequencies and the projection on the first environmental principal component [55]. We showed here that these correlations hold on our broad sample of 28 populations, with allele frequency at 115 (53%) SNPs correlating with environmental variation. As expected, the principal component driven by altitude (PCenv1) correlated to allele frequency for a greater fraction of SNPs than the second orthogonal component. Neither of them, however, displayed enrichment for SNPs associated with phenotypic variation. This observation conforms with the fact that correlation-based methods detect *between*-population divergence while phenotypic associations seek *within*-population variation. SNPs associated with environmental variation but not phenotypic variation, may indicate either that they were fixed – or almost fixed – within populations of

our association panel leading to low statistical power, or that the phenotype they influence was not measured. Conversely, SNPs associated to phenotypic but not to environmental variation may indicate either no environmental effect or the absence of the environmental driver from our variables. For example, it has been shown that soil is an important driver of local adaptation in teosintes [93], yet we did not quantify plant-soil interaction phenotypic traits, and neither did we evaluate soil variables. Finally, the subset of 87 (S5 Table, S11 Fig) outlier SNPs that are associated to both environmental and phenotypic variation point to situations where the SNP still segregates within populations and relates to measured phenotypes that are themselves associated to environmental driver(s) (PCenv1 and/or PCenv2). These genomic locations are likely of particular interest for ongoing adaptation.

Interestingly, we identified three Mb-scale inversions located on chromosomes 1 (*Inv1n*), 4 (*Inv4m*) and 9 (*Inv9e*) that, taken together, were enriched for SNPs associated with environmental variables related to altitude and/or phenotypic variation at multiple traits. Previous work [52,53] has shown that *Inv1n* and *Inv4m* segregate within both *parviglumis* and *mexicana*, while two inversions on chromosome 9, *Inv9d* and *Inv9e*, are present only in some of the highest *mexicana* populations; such that all four inversions also follow an altitudinal pattern. Our findings confirmed that three of these inversions possessed an excess of SNPs with high F_{st} between subspecies and between low- and high-*mexicana* populations for *Inv9e* [54]. Noteworthy *Inv9d* contains a large ear leaf width quantitative trait locus in maize [87]. Corroborating these results, we found consistent association between the only SNP located within this inversion and leaf width variation in teosinte populations (S5 Table). Overall, our results further strengthen the role of chromosomal inversions in teosinte altitudinal adaptation. Because they suppress recombination between inverted and non-inverted genotypes, their spread has likely contributed to the emergence and maintenance of

locally adaptive allelic combinations in the face of gene flow, not unlike a growing number of examples from other models (reviewed in [94]) including insects [95], fish [96], birds [97] and plants [98,99].

Conclusion.

Elevation gradients provide an exceptional opportunity for investigating variation of functional traits in response to continuous environmental factors at short geographical scales, where gene flow among populations is ongoing. Here we documented patterns indicating that local adaptation, likely facilitated by the existence of chromosomal inversions, allows teosintes to cope with specific environmental conditions. Using population genomic tools, we recovered variants that underlie adaptive phenotypic variation in teosintes. We also found evidence of pleiotropy (or of tightly linked genes) on phenotypic variation, which may impose genetic constraints and compromise the evolution of traits. Finally, we detected a number of SNPs associated with phenotypic variation of traits related to altitudinal adaptation. These traits are relevant for maize evolution and breeding. Whether the underlying SNPs detected in teosintes bear similar effects in maize, or whether their effects differ in domesticated backgrounds, will have to be further investigated.

Material and Methods

Description of teosinte populations and sampling.

We used 37 teosinte populations of *mexicana* (16) and *parviglumis* (21) subspecies from two previous collections [51,54,55] to design our sampling. These populations (S1 Table) are distributed along two altitudinal gradients (S1 Fig). We plotted their altitudinal profiles using R 'raster' package [100] (S2 Fig). We further obtained 19 environmental variable layers from http://idrisi.uaemex.mx/distribucion/superficies-climaticas-para-mexico. These high-resolution layers comprised monthly values from 1910 to 2009 estimated via interpolation methods [101]. We extracted values of the 19 climatic variables for each population (S1 Table).

We defined an association panel of 11 populations on which to perform a genotype-phenotype association study. Our choice was guided by grain availability as well as the coverage of the whole climatic and altitudinal ranges. Hence, we computed Principal Component Analyses (PCA) for each gradient from environmental variables using the FactoMineR package in R [102] and added altitude to the PCA graphs as a supplementary variable. Our association panel comprised five populations from a first gradient (*a*) – two *mexicana* and three *parviglumis*, and six populations from a second gradient (*b*) – one *mexicana* and five *parviglumis* (S1 Fig).

High throughput sequencing (HTS) data were obtained for six populations out of the 37 populations (M6a, P1a, M7b, P2b, M1b and P8b; S1 Fig, S1 Table) to detect candidate genomic regions for local adaptation [55]. The four highest and lowest of these populations are also included in our 11 common garden experiment populations.

Finally,we designed an extended sample of 28 populations to investigate correlation with environmental variation.

Common garden experiments

We used two common gardens for phenotypic evaluation of the association panel. Common gardens were located at INIFAP (Instituto Nacional de Investigaciones Forestales, Agricolas y Pecuaria) experimental field stations in the state of Guanajuato in Mexico, one in Celaya municipality at the Campo Experimental Bajío (CEBAJ) (20°31’20’’ N, 100°48’44’’W) at 1750 meters of elevation, and one in San Luis de la Paz municipality at the Sitio Experimental Norte de Guanajuato (SENGUA) (21°17’55’’N, 100°30’59’’W) at 2017 meters of elevation. These locations were selected because they present intermediate altitudes (S2 Fig) and environmental conditions where both lowland and highland populations could grow (S3 Fig). The two common gardens were replicated in 2013 and 2014.

The original sampling contained 15 to 22 mother plants per population. Eight to 12 grains per mother plant were sown each year in individual pots. After one month, seedlings were transplanted in the field. Each of the four fields (2 locations, 2 years) was separated into four blocks encompassing 10 rows and 20 columns. We evaluated one offspring of ~15 mother plants from each of the 11 teosinte populations in each block, using a semi-randomized design, i.e. each row containing one or two individuals from each population, and individuals being randomized within row, leading to a total of 2,640 individual teosinte plants evaluated.

Because grains were directly collected from wild populations, environmental maternal effects were not controlled for in our experiments. Such control would necessitate grain production from selfing of each plant in a system where inbreeding depression is likely very strong. We are therefore confounding here genetic and environmental maternal effects.

Genotyping of outlier SNPs

We extracted total DNA from each individual plant of the association panel as well as 20 individuals from each of the 18 remaining populations that were not included in the association panel (Table 1). Extractions were performed from 30 mg of lyophilized adult leaf material following recommendations of DNeasy 96 Plant Kit manufacturer (QIAGEN, Valencia, CA, USA). We genotyped SNPs using Kompetitive Allele Specific PCR technology (KASPar, LGC Group) [103].

Among SNPs identified as potentially involved in local adaptation, 270 were designed for KASPar assays, among which 218 delivered accurate quality data. Of the 218 SNPs, 141 were detected as outliers in two previous studies using a combination of statistical methods – including F_{st}-scans [104], Bayescan [29] and Bayenv2 [32,105], Bayescenv [106] – applied to either six of our teosinte populations [55] or to a broader set of 49 populations genotyped by the Illumina® MaizeSNP50 BeadChip [54]. The remaining outlier SNPs (77) were detected by F_{st}-scans from six populations (S1 Fig, S1 Table), following a simplified version of the rationale in [55] by considering only differentiation statistics: SNPs were selected if they displayed both a high differentiation (5% highest F_{st} values) between highland and lowland populations of both gradients, and a high differentiation (5% highest F_{st} values) between highland and lowland populations either within *parviglumis* (P2b and P8b) or within *mexicana* (M7b and M1b) or both, in gradient *b* (S1 Fig). In other words, we conditioned detection of outliers to repeated patterns in the two gradients, allele differentiation by altitude within one of the two subspecies, and avoided those fixed between the two subspecies.

SSR genotyping and genetic structuring analyses.

In order to quantify the population structure and individual kinship in our association panel, we genotyped 46 SSRs (S4 Table). Primers sequences are available from the maize database project [107] and genotyping protocol were previously published [108]. Genotyping was done at the GENTYANE platform (UMR INRA 1095, Clermont-Ferrand, France). Allele calling was performed on electropherograms with the GeneMapper® Software Applied Biosystems®. Allele binning was carried out using Autobin software [109], and further checked manually.

We employed STRUCTURE Bayesian classification software to compute a genetic structure matrix on individual genotypes. Individuals with over 40% missing data were excluded from analysis. For each number of clusters (K from 2 to 13), we performed 10 independent runs of 500,000 iterations after a burn-in period of 50,000 iterations, and combined these 10 replicates using the LargeKGreedy algorithm from the CLUMPP program [110]. We then used the Evanno method [111] to choose the optimal K value and plotted the resulting clusters using DISTRUCT software. We followed the same methodology to compute a structure matrix from the outlier SNPs.

We also inferred a kinship matrix from SSRs using SPAGeDI [112]. Kinship coefficients were calculated for each pair of individuals as correlation between allelic states [113]. Since teosintes are outcrossers and expected to exhibit an elevated level of heterozygosity, we estimated intra-individual kinship to fill in the diagonal. We calculated ten kinship matrices, each excluding the SSRs from one out of the 10 chromosomes.
Finally, we computed the pairwise linkage disequilibrium (LD) between the 178 outlier SNPs at a frequency > 5% using the R package LDcorSV [114] while correcting for the underlying structure and kinship estimated from SSRs [115]. SNP and microsatellite data are available at: XX.XXXX/XX.figshare.XXXXXXX .

Phenotypic trait measurements

We evaluated a total of 18 phenotypic traits in the association panel (S2 Table). We measured six traits related to plant architecture (PL: Plant Height, HLE: Height of the Lowest Ear, HHE: Height of the Highest Ear, Til: number of Tillers, LBr: number of Lateral Branches, NoE: number of Nodes with Ears), three traits related to leave morphologies (LeL: Leaf Length, LeW: Leaf Width, LeC: Leaf Color), three traits related to reproduction (MFT: Male Flowering date, FFT: Female Flowering date, TBr : Tassel Branching), five traits related to grains (Gr: number of Grains per ear, GrL: Grain Length, GrWi: Grain Width, GrWe: Grain Weight, GrC: Grain Color), and one trait related to Stomata (StD: Stomata Density). These traits were chosen because we suspected they could contribute to differences among teosinte populations based on a previous report of morphological characterization on 112 teosinte collections grown in five localities [116].

We measured the traits related to plant architecture and leaves after silk emergence. Grain traits were measured at maturity. Leaf and grain coloration were evaluated on a qualitative scale. For stomata density, we sampled three leaves per plant and conserved them in humid paper in plastic bags. Analyses were undertaken at the Institute for Evolution and Biodiversity (University of Münster) as followed: 5mm blade discs were cut out from the mid length of one of the leaves and microscopic images were taken after excitation with a 488nm laser. Nine locations (0.15mm^2) per disc were captured with 10 images per location along the z-axis (vertically along the tissue). We automatically filtered images based on quality and estimated leaf stomata density using custom image analysis algorithms implemented in Matlab. For each sample, we calculated the median stomata density over the (up to) nine locations. To verify detection accuracy, manual counts were undertaken for 54 random

samples. Automatic and manual counts were highly correlated (R^2=0.82), indicating reliable detection (see S1 Annex StomataDetection, Dittberner and de Meaux, for a detailed description). The filtered data set of phenotypic measurements is available at: XX.XXXX/XX.figshare.XXXXXXX.

Statistical analyses of phenotypic variation

In order to test for genetic effects on teosinte phenotypic variation, we decomposed phenotypic values of each trait considering a fixed population effect plus a random mother-plant effect (model M1):

$$Y_{ijklm} = \mu + \alpha_i + \beta_j + \theta_{ij} + \gamma_{k/ij} + \delta_l + P_{m/l} + \varepsilon_{ijklm} \qquad \text{(M1)}$$

where the response variable Y is the observed phenotypic value, μ is the total mean, α_i is the fixed year effect (i = 2013, 2014), β_j the fixed field effect (j is field station,*SENGUA, CEBAJ)*, θ_{ij} is the year by field interaction, $\gamma_{k/ij}$ is the fixed block effect (k = 1, 2, 3, 4) nested within the year-by-field combination, δ_l is the fixed effect of the population of origin (l = 1 to 11*)*, $P_{m/l}$ is the random effect of mother plant (m = 1 to 15) nested within population, and ε_{ijklm} is the individual residue. For the distribution of the effects, the same variance was estimated within-populations. All mixed models were run using ASReml v.3.0 [117], and fixed effects were tested through Wald tests.

For each trait, we represented variation among populations using box-plots on mean values per mother plant adjusted for the experimental design following model M'1

$$Y_{ijklm} = \mu + \alpha_i + \beta_j + \theta_{ij} + \gamma_{k/ij} + p_{m/l} + \varepsilon_{ijklm} \qquad \text{(M'1)}$$

where mother plant within population is considered as fixed. We used the function *predict* to obtain least-square means (ls-means) of each mother plant, and looked at the tendencies between population's values.

We performed a principal component analysis (PCA) on phenotypic values corrected for the experimental design, using FactoMineR package in R [102] from the residues of model M2 computed using the *lm* package in R:

$$Y_{ijklm} = \mu + \alpha_i + \beta_j + \theta_{ij} + \gamma_{k/ij} + \varepsilon_{ijklm} \quad \text{(M2)}$$

Finally, we tested for altitudinal effects on traits by considering the altitude of the sampled population (*l*) as a covariate (ALT) in model M3.

$$Y_{ijklm} = \mu + \alpha_i + \beta_j + \theta_{ij} + \gamma_{k/ij} + P_{m/l} + a \cdot ALT_l + \varepsilon_{ijklm} \quad \text{(M3)}$$

Where all the terms are equal to those in model M1 except that the fixed effect of the population of origin, that was replaced by a regression on the population altitude (ALT_l).

We aimed at detecting traits evolving under spatially varying selection by comparing phenotypic to neutral genotypic differentiation. Q_{st} is a statistic analogous to F_{st} but for quantitative traits, which can be described as the proportion of phenotypic variation explained by differences among populations [19,118]. Significant differences between Q_{st} and F_{st} can be interpreted as evidence for spatially-varying ($Q_{st}>F_{st}$) selection [118]. We used the R package *QstFstComp* [119] that is adequate for experimental designs with randomized half-sibs in outcrossing species. We established a distribution of the difference between statistics (Q_{st}-F_{st}) under neutral hypothesis using the half-sib dam breeding design and 1000 resamples, and compared it to the observed difference using a 95% threshold cutoff value in order to detect traits under spatially-varying selection.

Q_{st} estimates relied on the assumption that the observed phenotypic variation was determined by additive genotypic variation. We thus estimated narrow-sense heritability for each trait in each population to estimate the proportion of additive variance in performance. We calculated per population narrow-sense heritabilites as the ratio of the estimated additive genetic variance over the total phenotypic variance on our common garden measurements

using the MCMCglmm R package [120] where half sib family is the single random factor, and the design (block nested within year and field) is corrected as fixed factor. For three grain-related traits, we also ran the same model but including mother plants phenotypic values calculated from the remaining grains not sown. We ran 100,000 iterations with 10,000 burn-in, inverse gamma (0.001; 0.001) as priors. We then calculated the mean and standard deviation of the 11 per population h^2 estimates.

Pairwise correlations between traits.

We evaluated pairwise-correlations between traits by correlating the residues obtained from model M4, that corrects for the underlying genetic structure as estimated from SSRs:

$$Y_{ijklm} = \mu + \alpha_i + \beta_j + \theta_{ij} + \gamma_{ijk} + \sum_{n=1}^{4} b_n C^n_{ijklm} + \varepsilon_{ijklm} \quad \text{(M4)}$$

where b_n is the fixed effect of the structure covariate C^n. Membership values for the C^n covariates were calculated at the individual level, i.e. for each offspring of mother plant *m* from population *l*, grown in the year *i* field *j* and block *k*. C^n is thus declared within *ijkl* indices, although purely genetic covariants.

We further considered the four year-field experimental environments as independent, and used blocks as replicates within year-field. We obtained 16 Pearson correlation values for each pair of traits (four per year-field treatment). We retained correlation values calculated with >7 data points. We then used R values as response variables in a linear model (M5) that considered a fixed population (δ) and year-field ($\alpha_i + \beta_j + \theta_{ij}$) effects, and their interaction (φ):

$$R_{ijlk} = \mu + \alpha_i + \beta_j + \theta_{ij} + \delta_l + \varphi_{ijl} + \varepsilon_{ijlk} \quad \text{(M5)}$$

For all linear models, we visually checked assumptions of independence and normally distributed residues.

Association mapping

We tested the association of phenotypic measurements with outlier SNPs on a subset of individuals for which (1) phenotypic measurements were available, (2) at least 60% of outlier SNPs were adequately genotyped, and (3) kinship and cluster membership values were available from SSR genotyping. For association, we removed SNPs with minor allele frequency lower than 5%.

In order to detect statistical associations between outlier SNPs and phenotypic variation, we used the following mixed model derived from [121]:

$$Y_{ijklom} = \mu + \alpha_i + \beta_j + \theta_{ij} + \gamma_{ijk} + \sum_{n=1}^{4} b_n \cdot C^n_{ijkolm} + \zeta_o + u_{ijklm} + \varepsilon_{ijklom} \quad \text{(M6)}$$

where ζ is the fixed bi-allelic SNP factor effect with one level for each of the three genotypes (o=1, 2, 3; with o=2 for heterozygous individuals,), u_{ijklom} being the random genetic effect of each individual. We assumed that the vector of u_{ijklom} followed a $N(0,K\sigma^2u)$ distribution, where K is the inversed kinship matrix.

The model was implemented in ASReml v.3.0 [117] in R and run for each SNP independently. In order to avoid overcorrection of neutral genetic structure and improve power, we ran the model independently for each chromosome using a kinship matrix estimated from all SSRs except those contained in the chromosome tested [122]. We tested SNP effects though the Wald statistics provided by ASReml, and applied 5% False Discovery Rate (FDR) thresholds for each phenotype separately. We generated Qqplots using 38 SSRs for each of the 18 traits. To this purpose, multiallelic genotypes were transformed to biallelic genotypes filtered for MAF > 5% and ran associations with the complete M6 model as well as the M6 model with either excluding kinship or structure and kinship.

Finally, we tested for correlation between the excess of common associated SNPs between two traits, and the absolute value of their pairwise phenotypic correlation. We computed both parametric (Pearson coefficient) and non-parametric (Kendall coefficient) correlation (Fig 6B). We calculated the excess of common associated SNPs as the difference between observation and expectation – under the hypothesis that the proportion of associated SNPs is independent between traits.

Environmental correlation of outlier SNPs

We tested associations between allelic frequency at 218 outlier SNPs and environmental variables using Bayenv 2.0 [37,105]. Because environmental variables are highly correlated, we used the first two principal component axis from the environmental PCA analysis (PCenv1 and PCenv2) to run Bayenv 2.0. This software requires a neutral covariance matrix, that we computed from an available dataset of SNPs [54] for 28 popualtions (S1 Table). We consequently restricted our analysis to 28 populations. From this available dataset, we randomly extracted 1000 SNPs found to display no selection footprint, hereafter neutral SNPs [54]. Genotypes were available for 24 to 34 individuals per population, albeit different from the ones of our association mapping panel. We employed these neutral SNPs to compute a population correlation matrix in Bayenv 2.0 by running 100,000 iterations and saving the matrix every 500 iterations. We then tested the correlation of these to the last matrix obtained as well as with an *Fst* matrix calculated using BEDASSLE [123], as described in [54].

For each outlier SNP, we compared the posterior probability of a model that included an environmental factor (PCenv1 or PCenv2) to a null model. We determined a 5% threshold for significance of environmental association by running 100,000 iterations on neutral SNPs.

We carried out five independent runs for each outlier SNP and evaluated their consistency from the coefficient of variation of the Bayes factors calculated among runs.

Acknowledgments

We thank Jessica Melique for her help in gathering stomata data. We are very grateful to Angelica Cibrian at Langebio (Cinvestav, Irapuato, Mexico) who let us use her lab to lyophilize our samples, and store them. Valeria Souza greatly helped us with logistic support in Mexico. Insights from Delphine Legrand were extremely precious for analyzing correlations between traits.

Funding

This work was supported by two grants overseen by the French National Research Agency (ANR) (Project ANR 12-ADAP-0002-01) to MIT and YV, and the ECOSNord/ANUIES/CONACYT/SEP project M12A03, CONACYT-ANUIES 207571 to MIT and LEE. LEE research and JAA-L and M-AF postdoctoral salaries were supported by CONACYT-Mexico Investigación Científica Básica CB2011/167826 awarded to LEE. M-AF was funded by the Project ANR 12-ADAP-0002-01 and NEM-A was funded by a CONACYT PhD fellowship grant no. 579966/410748.

Author contributions

Conceived and designed the experiments: MIT, DM. Contributed plant material: LEE, JAA-L, SM, MIT. DNA extractions: HC, AR, M-AF, DM. Conducted field experiments and performed phenotypic measurements: M-AF, MIT, MGC, SM. Outlier SNP detection: M-AF. Microsatellite genotyping: AV, HC, FD, MF. Neutral SNP genotyping: LEE, JAA-L. Stomata density images and pipeline: JdD, HD. Statistical methodology: LM, MIT, DM, M-AF, NEM-A. Implemented methods, wrote scripts: M-AF, NEM-A. Analyzed the data: M-AF, NEM-A. Prepared Tables and Figures: M-AF, NEM-A. Discussed interpretations: M-AF, NEM-A, DG, LM, JdM, YV, DM, MIT. Wrote the paper: NEM-A, M-AF, MIT. Corrected and commented the manuscript: all authors.

Supporting information captions

SUPPLEMENTARY FIGURES

Figure S1: Geographical location of the 37 populations. *parviglumis* (circles) and *mexicana* (triangles) populations were sampled along gradient *a* (gray) and gradient *b* (black) in Mexico. The 11 populations indicated with a purple outline constituted our association panel.

Figure S2: Altitudinal profiles along gradients *a* and *b*. Sampled populations are plotted on parallel altitudinal profiles for gradients *a* and *b*. Darker gray lines indicate lower latitude for gradient *a* and lower longitude for gradient *b*. Sampled populations are plotted by green circles (*parviglumis*) or red triangles (*mexicana*). The altitude of the two experimental fields (CEBAJ: 1750m and SENGUA: 2017m) are marked with stars on y-axes.

Figure S3: Principal Component Analysis of 19 climate variables for 37 teosinte populations. A: Projection of *parviglumis* (green circles) and *mexicana* (red triangles) populations on the first PCA plane with gradients *a* and *b* indicated by triangles and circles respectively. The 11 populations evaluated in common gardens are surrounded by a purple outline. Populations that were previously sequenced to detect selection footprints are shown in bold (S1 Table). B: Correlation circle of the 19 climatic variables on the first PCA plane. Climatic variables indicated as Tn (n from 1 to 11) and Pn (n from 12 to 19) are related to temperature and precipitation, respectively. Altitude (in blue) was added as a supplementary variable.

Figure S4: Box-plots of adjusted means by field, year and block, for all traits. Populations are ranked by altitude. *parviglumis* populations are shown in green and *mexicana* in red. Lighter colors are used for gradient 'a' and darker colors for gradient 'b'. Units of measurement correspond to those defined in S2 Table. For male and female flowering time, we report values for all 11 populations although very few individuals from the two most lowland populations (P1a and P2b) flowered. Covariation with altitude was significant for all traits except for the number of nodes with ears on the main tiller (S3 Table).

Figure S5: Genomic F_{st}-scans on 6 teosinte populations. We computed 4 pairwise-F_{st} values from 6 populations previously sequenced (S1 Table). Those include F_{st} between lowland and highland populations of each gradient (P1a-M6a, P2b-M7b) as well as within subspecies on gradient *b* (P2b-P8b, M1b-M7b). F_{st} values are averaged across sliding windows of 20 SNPs with a step of five SNPs (from top to bottom, chromosome 1 to 10) and normalized across pairwise comparisons to facilitate vizualisation. Only the top 1% values are represented. The 1‰ thresholds for each pairwise comparisons are indicated by colored horizontal lines. Horizontal black bars indicate location of inversions on chromosome 1 (*Inv1n*), chromosome 4 (*Inv4m*) and chromosome 9 (*Inv9d*). The subset of 218 outlier SNPs analyzed in the present study is indicated with black tick marks along the X axes.

Figure S6: Pairwise Linkage Disequilibrium (LD) between outlier SNPs. Pairwise LD between 178 SNPs was estimated using r^2, and corrected for structure and kinship computed from 38 SSRs.

Figure S7: QQ-plots of observed P-values and expected P-values generated from 38 SSRs. We employed three versions o the model M6 with different types of corrections for genetic strucutre and kinship.

Figure S8: Manhattan plots of association between 178 outlier SNPs and 14 phenotypic traits. X-axis indicates the position of outlier SNPs on chromosomes 1 to 10 (black and gray colors alternating). The red line indicates significance thresholds with associated SNPs above those lines colored accordingly.

Figure S9: Significant effects of year-field, population and their interaction on phenotypic correlations. Pairwise correlations between phenotypic traits were computed as in Fig 6. The squares surrounding the correlations denote significant effects recovered from the M5 model where correlation values were considered as response variables. Note that a correlation may not be significant considering data from all populations and environments together, yet we may observe significant correlations when calculated by year-field or population.

Figure S10: Venn diagram of SNPs associated to phenotypic variation and SNPs whose allele frequencies correlated to environmental PCs (PCenv1 and PCenv2). The 165 SNPs that displayed either association with phenotypes (Pheno) and/or environmental correlations to PCenv1 and PCenv2 are shown on the diagram.

Figure S11: Manhattan plots of association between 178 outlier SNPs and 18 phenotypic traits along with their Bayenv2 outlier status for PCenv1. X-axis indicates the position of

SNPs on chromosomes 1 to 10 (black and gray colors alternating). The dotted red line indicates significance threshold for phenotypic association. SNPs are colored in red when they were significantly associated with the phenotypic variation, in purple when they were additionally associated to PCenv1. Below the threshold, SNPs in sky blue are those associated to environmental PCenv1 but not to phenotypes.

SUPPLEMENTARY TABLES

S1 Table. Description of 37 teosinte populations and sets of populations used in the present study by data types.

S2 Table. List of the 18 phenotypic traits measured and estimates of narrow-sense heritabilities (h^2).

S3 Table. Significance of main effects for each trait as determined by models M1 and M3.

S4 Table. Description of 46 SSRs and genotyping success rate.

S5 Table. Characteristics, association with phenotypes and correlation with environment of 218 outlier SNPs.

S6 Table. Number of individuals used to test associations between 178 SNPs and 18 phenotypes.

References

1. Whitlock MC. Modern approaches to local adaptation. Am Nat. 2015;186(october).
2. Lande R. Natural selection and random genetic drift in phenotypic evolution. Evolution. 1976;30(2):314–34.
3. Bulmer M. G. Multiple niche polymorphism. Am Nat. 1972;106(948):254–7.
4. Gay L, Crochet PA, Bell DA, Lenormand T. Comparing clines on molecular and phenotypic traits in hybrid zones: A window on tension zone models. Evolution. 2008;62(11):2789–806.
5. Lenormand T. Gene flow and the limits to natural selection. Trends in Ecology and Evolution. 2002.
6. Whitlock MC, Gomulkiewicz R. Probability of fixation in a heterogeneous environment. Genetics. 2005;1–40.
7. Yeaman S, Otto SP. Establishment and maintenance of adaptive genetic divergence under migration, selection and drift. Evolution. 2011;67(7):2123–9.
8. Bradshaw AD. Ecological significance of genetic variation between populations. In: Dirzo R, Sarukhan J, editors. Perspectives on plant population ecology. Sunderland, MA.: Sinauer; 1984. p. 213–228.
9. Endler JA. Natural selection in the wild. Monographs. Princeton, N.J: Princeton University Press; 1986. 354 p.
10. Rundle HD, Nosil P. Ecological speciation. Ecol Lett. 2005;8:336–52.
11. Kawecki TJ, Ebert D. Conceptual issues in local adaptation. Vol. 7, Ecology Letters. 2004. p. 1225–41.
12. Hereford J. A Quantitative Survey of Local Adaptation and Fitness Trade□Offs. Am Nat. 2009;
13. Leimu R, Fischer M. A meta-analysis of local adaptation in plants. PLoS One. 2008;3(12).
14. Tiffin P, Ross-Ibarra J. Advances and limits of using population genetics to understand local adaptation. Trends Ecol Evol. 2014;29(12):673–80.
15. Garcia-Ramos G, Kirkpatrick M. Genetic models of adaptation and gene flow in peripherial populations. Evolution. 1997;51(I):21–8.
16. Slatkin M. Rare alleles as indicators of gene flow. Evolution. 1985;39(1):53–65.

17. Lande R. Neutral theory of quantitative genetic variance in an island model with local extinction and colonization. Evolution. 1992;46(2):381–9.

18. Whitlock MC. Neutral additive genetic variance in a metapopulation. Genet Res. 1999;74:215–21.

19. Spitze K. Population structure in Daphina obtusa: quantitative genetic and allozymic variation. Genet Soc Am. 1993;135:367–74.

20. Wright S. The genetical structure of populations. Ann Eugen. 1951;15(1):323–54.

21. Luquet E, Léna J-P, Miaud C, Plénet S. Phenotypic divergence of the common toad (*Bufo bufo*) along an altitudinal gradient: evidence for local adaptation. Heredity. 2015;114(1):69–79.

22. Roschanski AM, Csilléry K, Liepelt S, Oddou-Muratorio S, Ziegenhagen B, Huard F, et al. Evidence of divergent selection for drought and cold tolerance at landscape and local scales in *Abies alba* Mill. in the French Mediterranean Alps. Mol Ecol. 2016;25(3):776–94.

23. Kawakami T, Morgan TJ, Nippert JB, Ocheltree TW, Keith R, Dhakal P, et al. Natural selection drives clinal life history patterns in the perennial sunflower species, *Helianthus maximiliani*. Mol Ecol. 2011;20(11):2318–28.

24. Moyers BT, Rieseberg LH. Remarkable life history polymorphism may be evolving under divergent selection in the silverleaf sunflower. Mol Ecol. 2016;25(16):3817–30.

25. Bierne N, Welch J, Loire E, Bonhomme F, David P. The coupling hypothesis: Why genome scans may fail to map local adaptation genes. Mol Ecol. 2011;20(10):2044–72.

26. Lewontin RC, Krakauer J. Distribution of gene frequency as a test of the theory of the selective neutrality of polymorphisms. Genetics. 1973;74(1):175–95.

27. Beaumont MA, Nichols RA. Evaluating loci for use in the genetic analysis of population structure. Proc R Soc B Biol Sci. 1996;263(1377):1619–26.

28. Vitalis R, Dawson K, Boursot P. Interpretation of variation across marker loci as evidence of selection. Genetics. 2001;158(4):1811–23.

29. Foll M, Gaggiotti O. A genome scan method to identify selected loci appropriate for both dominant and codominant markers: A Bayesian perspective. Genetics. 2008;180(2):977–93.

30. Excoffier L, Hofer T, Foll M. Detecting loci under selection in a hierarchically structured population. Heredity. 2009;103(4):285–98.

31. Bonhomme M, Chevalet C, Servin B, Boitard S, Abdallah J, Blott S, et al. Detecting selection in population trees: The Lewontin and Krakauer test extended. Genetics. 2010;186(1):241–62.

32. Günther T, Coop G. Robust identification of local adaptation from allele frequencies. Genet Soc Am. 2013;195(September):205–20.

33. Lotterhos KE, Whitlock MC. Evaluation of demographic history and neutral parameterization on the performance of FST outlier tests. Mol Ecol. 2014;23(9):2178–92.

34. Haasl RJ, Payseur BA. Fifteen years of genomewide scans for selection: trends, lessons and unaddressed genetic sources of complication. Mol Ecol. 2016;25(1):5–23.

35. Le Corre V, Kremer A. The genetic differentiation at quantitative trait loci under local adaptation. Mol Ecol. 2012;21(7):1548–66.

36. Yi X, Liang Y, Huerta-Sanchez E, Jin X, Xi Ping Cuo Z, Pool JE, et al. Sequencing of fifty human exomes reveals adaptations to high altitude. Science. 2010;329(5987):75–8.

37. Coop G, Witonsky D, Di Rienzo A, Pritchard JK. Using environmental correlations to identify loci underlying local adaptation. Genetics. 2010;

38. Guillot G, Renaud S, Ledevin R, Michaux J, Claude J. A unifying model for the analysis of phenotypic, genetic, and geographic data. 2012;61(5):897–911.

39. Frichot E, Schoville SD, Bouchard G, Franc O. Testing for Associations between Loci and Environmental Gradients Using Latent Factor Mixed Models. Mol Biol Evol. 2013;30(7):1687–99.

40. Gautier M. Genome-wide scan for adaptive divergence and association with population-specific covariates. Genetics. 2015;201(4):1555–79.

41. Joost S, Bonin A, Bruford MW, Després L, Conord C, Erhardt G, et al. A spatial analysis method (SAM) to detect candidate loci for selection: Towards a landscape genomics approach to adaptation. Mol Ecol. 2007;16(18):3955–69.

42. Poncet BN, Herrmann D, Gugerli F, Taberlet P, Holderegger R, Gielly L, et al. Tracking genes of ecological relevance using a genome scan in two independent regional population samples of *Arabis alpina*. Mol Ecol. 2010;19(14):2896–907.

43. De Mita S, Thuillet AC, Gay L, Ahmadi N, Manel S, Ronfort J, et al. Detecting selection along environmental gradients: Analysis of eight methods and their effectiveness for outbreeding and selfing populations. Mol Ecol. 2013;22(5):1383–99.

44. Hoban S, Kelley JL, Lotterhos KE, Antolin MF, Bradburd G, Lowry DB, et al. Finding the genomic basis of local adaptation: pitfalls, practical solutions, and future directions. Am Nat [Internet]. 2016;188(4):379–97.

45. De Villemereuil P, Frichot É, Bazin É, François O, Gaggiotti OE. Genome scan methods against more complex models: When and how much should we trust them? Mol Ecol. 2014;23(8):2006–19.

46. Fournier-Level A, Korte A, Cooper MD, Nordborg M, Schmitt J, Wilczek AM. A map of local adaptation in *Arabidopsis thaliana*. Science. 2011;334(6052):86–9.

47. Hancock AM, Brachi B, Faure N, Horton MW, Jarymowycz LB, Sperone FG, et al. Adaptation to climate across the Arabidopsis thaliana genome. Science. 2011;334(October):83–6.

48. Ross-Ibarra J, Tenaillon M, Gaut BS. Historical divergence and gene flow in the genus *Zea*. Genetics. 2009;181(4):1399–413.

49. Hufford MB, Martínez-Meyer E, Gaut BS, Eguiarte LE, Tenaillon MI. Inferences from the historical distribution of wild and domesticated maize provide ecological and evolutionary insight. PLoS One. 2012;7(11).

50. Bilinski P, Albert PS, Berg JJ, Birchler JA, Grote MN, Lorant A, et al. Parallel altitudinal clines reveal trends in adaptive evolution of genome size in *Zea mays*. PLoS Genet. 2018;14(5).

51. Diez CM, Gaut BS, Meca E, Scheinvar E, Montes-Hernandez S, Eguiarte LE, et al. Genome size variation in wild and cultivated maize along altitudinal gradients. New Phytol. 2013;199(1):264–76.

52. Pyhäjärvi T, Hufford MB, Mezmouk S, Ross-Ibarra J. Complex patterns of local adaptation in teosinte. Genome Biol Evol. 2013;5(9):1594–609.

53. Fang Z, Pyhäjärvi T, Weber AL, Dawe RK, Glaubitz JC, Sánchez González J de J, et al. Megabase-scale inversion polymorphism in the wild ancestor of maize. Genetics. 2012;191(3):883–94.

54. Aguirre-Liguori JA, Tenaillon MI, Vázquez-Lobo A, Gaut BS, Jaramillo-Correa JP, Montes-Hernandez S, et al. Connecting genomic patterns of local adaptation and niche suitability in teosintes. Mol Ecol. 2017;

55. Fustier MA, Brandenburg JT, Boitard S, Lapeyronnie J, Eguiarte LE, Vigouroux Y, et al. Signatures of local adaptation in lowland and highland teosintes from whole-genome sequencing of pooled samples. Mol Ecol. 2017;26:2738–56.

56. Sohail M, Maier RM, Ganna A, Bloemendal A, Martin AR, Turchin MC, et al. Signals of polygenic adaptation on height have been overestimated due to uncorrected population structure in genome-wide association studies. bioRxiv. 2018;355057.

57. Kronholm I, Loudet O, de Meaux J. Correction: Influence of mutation rate on estimators of genetic differentiation - lessons from *Arabidopsis thaliana*. BMC Genet. 2010;11:7–9.

58. Halbritter AH, Fior S, Keller I, Billeter R, Edwards PJ, Holderegger R, et al. Trait differentiation and adaptation of plants along elevation gradients. J Evol Biol. 2018;31(6):784–800.

59. Körner C. The use of “altitude” in ecological research. Trends Ecol Evol. 2007;22(11):569–74.

60. Friend AD, Woodward FI, Switsur VR. Field measurements of photosynthesis, stomatal conductance, leaf nitrogen and δ 13 C along altitudinal gradients in Scotland. Funct Ecol. 1989;3(1):117.

61. Neuner G. Frost resistance in alpine woody plants. Front Plant Sci. 2014;5(December).

62. Frohnmeyer H, Staiger D. Update on ultraviolet-B light responses ultraviolet-B radiation-mediated responses in plants. Balancing damage and protection. 2014;133(December):1420–8.

63. Byars SG, Papst W, Hoffmann AA. Local adaptation and cogradient selection in the alpine plant, *Poa hiemata*, along a narrow altitudinal gradient. Evolution. 2007;61(12):2925–41.

64. Luo Y, Widmer A, Karrenberg S. The roles of genetic drift and natural selection in quantitative trait divergence along an altitudinal gradient in Arabidopsis thaliana. Heredity. 2015;

65. Guerin GR, Wen H, Lowe AJ, Guerin GR, Wen H. Leaf morphology shift linked to climate change. Popul Ecol. 2012;(July):882–6.

66. Kofidis G, Bosabalidis AM, Moustakas M. Contemporary seasonal and altitudinal variations of leaf structural features in oregano (*Origanum vulgare* L.). Ann Bot. 2003;92(5):635–45.

67. Mendez-Vigo B, Pico FX, Ramiro M, Martinez-Zapater JM, Alonso-Blanco C. Altitudinal and climatic adaptation is mediated by flowering traits and FRI, FLC, and PHYC genes in *Arabidopsis*. Plant Physiol. 2011;157(4):1942–55.

68. Oleksyn J, Modrzynski J, Tjoelker MG, Zytkowaik R, Reich PB, Karolewski P. Growth and physiology of *Picea abies* populations from elevational transects: common garden evidence for altitudinal ecotypes and cold adaptation. 1998;573–90.

69. Doebley JF. Maize introgression into teosinte -- a reappraisal. Ann Missouri Bot Gard. 1984;71:1100–13.

70. Lauter N, Gustus C, Westerbergh A, Doebley J. The inheritance and evolution of leaf pigmentation and pubescence in teosinte. Genet Soc Am. 2004;167(August):1949–59.

71. Raven, John A. Selection pressures on stomatal evolution. New Phytol. 2002;153(3):371–86.

72. Dittberner H, Korte A, Mettler-Altmann T, Weber APM, Monroe G, de Meaux J. Natural variation in stomata size contributes to the local adaptation of water-use efficiency in *Arabidopsis thaliana*. Mol Ecol. 2018;1–40.

73. Carlson JE, Adams CA, Holsinger KE. Intraspecific variation in stomatal traits, leaf traits and physiology reflects adaptation along aridity gradients in a South African shrub. Ann Bot. 2016;117(1):195–207.

74. Körner C, Mayr R. Stomatal behaviour in alpine plant communities between 600 and 2600 metres above sea level. In: Grace J, Ford ED, Jarvis PG, editors. Plants and their Atmospheric Environment. Blackwell, Oxford,; 1981. p. pp 205–218.

75. Bresson CC, Vitasse Y, Kremer A, Delzon S. To what extent is altitudinal variation of functional traits driven by genetic adaptation in European oak and beech? Tree Physiol. 2011;31(11):1164–74.

76. Körner C, Neumayer M, Menendez-Riedl SP, Smeets-Scheel A. Functional morphology of mountain plants. Flora. 1989;182(5–6):353–83.

77. Smith JSC, Goodman MM, Lester RN. Variation within teosinte. I. Numerical analysis of morphological data. Econ Bot. 1981;35(2):187–203.

78. Jakobsson A, Eriksson O. A comparative study of seed number , seed size , seedling size and recruitment in grassland plants. Oikos. 2000;88:494–502.

79. Buckler ES, Holland JB, Bradbury PJ, Acharya CB, Brown PJ, Browne C, et al. The genetic architecture of maize flowering time. Science. 2009;325(7):714–8.

80. Moreau L, Charcosset A, Gallais A. Use of trial clustering to study QTL x environment effects for grain yield and related traits in maize. Theor Appl Genet. 2004;110(1):92–105.

81. Durand E, Bouchet S, Bertin P, Ressayre A, Jamin P, Charcosset A, et al. Flowering time in maize: Linkage and epistasis at a major effect locus. Genetics. 2012;190(4):1547–62.

82. Li D, Wang X, Zhang X, Chen Q, Xu G, Xu D, et al. The genetic architecture of leaf number and its genetic relationship to flowering time in maize. New Phytol. 2015;210(1):256–68.

83. Weber AL, Briggs WH, Rucker J, Baltazar BM, Sánchez-Gonzalez JDJ, Feng P, et al. The genetic architecture of complex traits in teosinte (*Zea mays* ssp. *parviglumis*): New evidence from association mapping. Genetics. 2008;180(2):1221–32.

84. Pritchard JK, Pickrell JK, Coop G. The genetics of human adaptation: hard sweeps, soft sweeps, and polygenic adaptation. Curr Biol. 2010;20(4):R208–15.

85. Tian F, Bradbury PJ, Brown PJ, Hung H, Sun Q, Flint-Garcia S, et al. Genome-wide association study of leaf architecture in the maize nested association mapping population. Nat Genet. 2011;43(2):159–62.

86. Simons YB, Bullaughey K, Hudson RR, Sella G. A population genetic interpretation of GWAS findings for human quantitative traits. PLoS Biol. 2018;16(3).

87. Yu J, Li X, Zhu C, Yeh C-T, Wu W, Takacs E, et al. Genic and non-genic contributions to natural variation of quantitative traits in maize. Genome Res. 2012;2436–44.

88. Hung H-Y, Shannon LM, Tian F, Bradbury PJ, Chen C, Flint-Garcia SA, et al. ZmCCT and the genetic basis of day-length adaptation underlying the postdomestication spread of maize. Proc Natl Acad Sci. 2012;109(28):E1913–21.

89. Whitt SR, Wilson LM, Tenaillon MI, Gaut BS, Buckler ES. Genetic diversity and selection in the maize starch pathway. Proc Natl Acad Sci U S A. 2002;99(20):12959–62.

90. Jaenicke-Després V, Buckler ES, Smith BD, Gilbert MTP, Cooper A, Doebley J, et al. Early allelic selection in maize as revealed by ancient DNA. Science. 2003;302(5648):1206–8.

91. Corbi J, Debieu M, Rousselet A, Montalent P, Le Guilloux M, Manicacci D, et al. Contrasted patterns of selection since maize domestication on duplicated genes encoding a starch pathway enzyme. Theor Appl Genet. 2011;122(4):705–22.

92. Hannah LC, Futch B, Bing J, Shaw JR, Boehlein S, Stewart JD, et al. A shrunken-2 transgene increases maize yield by acting in maternal tissues to increase the frequency of seed development. Plant Cell. 2012;24(6):2352–63.

93. O'Brien AM, Sawers RJH, Strauss SY, Ross-Ibarra J. Adaptive phenotypic divergence in teosinte differs across biotic contexts. 2018;

94. Wellenreuther M, Bernatchez L. Eco-evolutionary genomics of chromosomal inversions. Trends in Ecology and Evolution. 2018.

95. Ayala D, Ullastres A, González J. Adaptation through chromosomal inversions in *Anopheles*. Front Genet. 2014;5(MAY):1–10.

96. Barth JMI, Berg PR, Jonsson PR, Bonanomi S, Corell H, Hemmer-Hansen J, et al. Genome architecture enables local adaptation of Atlantic cod despite high connectivity. Mol Ecol. 2017;26(17):4452–66.

97. Lundberg M, Liedvogel M, Larson K, Sigeman H, Grahn M, Wright A, et al. Genetic differences between willow warbler migratory phenotypes are few and cluster in large haplotype blocks. Evol Lett. 2017;155–68.

98. Twyford AD, Friedman J. Adaptive divergence in the monkey flower *Mimulus guttatus* is maintained by a chromosomal inversion. Evolution. 2015;69(6):1476–86.

99. Lowry DB, Willis JH. A widespread chromosomal inversion polymorphism contributes to a major life-history transition, local adaptation, and reproductive isolation. PLoS Biol. 2010;8(9).

100. Hijmans RJ, van Etten J, Cheng J, Mattiuzzi M, Sumner M, Greenberg JA, et al. Package ‘raster ’: geographic data analysis and modeling. 2018;242.

101. Cuervo-Robayo AP, Téllez-Valdés O, Gómez-Albores MA, Venegas-Barrera CS, Manjarrez J, Martínez-Meyer E. An update of high-resolution monthly climate surfaces for Mexico. Int J Climatol. 2014;34(7):2427–37.

102. Husson F, Josse J, Le S, Mazet J. Package ‘ FactoMineR ’. An R package. 2016;(1):96.

103. Semagn K, Babu R, Hearne S, Olsen M. Single nucleotide polymorphism genotyping using Kompetitive Allele Specific PCR (KASP): Overview of the technology and its application in crop improvement. Mol Breed. 2014;33(1):1–14.

104. Weir BS, Hill WG. Estimating F-statistics. Annu Rev Genet. 2002;36:721–50.

105. Günther T, Coop G. A Short Manual for Bayenv2.0. 2016;

106. de Villemereuil P, Gaggiotti OE. A new FST-based method to uncover local adaptation using environmental variables. Methods Ecol Evol. 2015;

107. Andorf CM, Cannon EK, Portwood JL, Gardiner JM, Harper LC, Schaeffer ML, et al. MaizeGDB update: New tools, data and interface for the maize model organism database. Nucleic Acids Res. 2016;44(D1):D1195–201.

108. Camus-Kulandaivelu L, Veyrieras JB, Madur D, Combes V, Fourmann M, Barraud S, et al. Maize adaptation to temperate climate: Relationship between population structure and polymorphism in the Dwarf8 gene. Genetics. 2006;172(4):2449–63.

109. Guichoux E, Lagache S, Wagner S, Chaumeil P, Léger P, Lepais O, et al. Current trends in microsatellite genotyping. Mol Ecol Resour. 2011;11:591–611.

110. Jakobsson M, Rosenberg NA. CLUster Matching and Permutation Program Version 1.1.2. 2007;

111. Evanno G, Regnaut S, Goudet J. Detecting the number of clusters of individuals using the software STRUCTURE: A simulation study. Mol Ecol. 2005;14(8):2611–20.

112. Hardy OJ, Vekemans X. spagedi: a versatile computer program to analyse spatial genetic structure at the individual or population levels. Mol Ecol Notes. 2002;2:618–20.

113. Loiselle BA, Sork VL, Nason JD, Graham C. Spatial genetic structure of a tropical understory shrub, *Psychotria officinalis* (Rubiaceae). Am J Bot. 1995;82(11):1420–5.

114. Desrousseaux AD, Sandron F, Siberchicot A, Cierco-Ayrolles C, Mangin B. Package ‘ LDcorSV.’ 2017;

115. Mangin B, Siberchicot A, Nicolas S, Doligez A, This P, Cierco-Ayrolles C. Novel measures of linkage disequilibrium that correct the bias due to population structure and relatedness. Heredity. 2012;108(3):285–91.

116. Sanchez J de J, Kato Yamakake TA, Aguilar Sanmiguel M, Hernandez Casillas JM, Lopez Rodriguez A, Ruiz Corral JA. Distribucion y caracterización del teocintle. Guadalajara, Jalisco, Mexico: Centro de Investigacion Regional del Pacifico Centro, INIFAP, SAGAR; 1998. 165 p.

117. Butler D, Cullis BR, Gilmour AR, Gogel BJ. for S language environments ASReml-R reference manual. Fish. 2007;(February).

118. Holsinger KE, Weir BS. Genetics in geographically structured populations: defining, estimating and interpreting F(ST). Nat Rev Genet. 2009;10(September):639–50.

119. Gilbert KJ, Whitlock MC. QST-FST comparisons with unbalanced half-sib designs. Mol Ecol Resour. 2015;15(2):262–7.

120. Hadfield JD. MCMC methods for multi-response generalized linear mixed models: the MCMCglmm R package. J Stat Softw. 2010;33(2).

121. Yu J, Pressoir G, Briggs WH, Vroh Bi I, Yamasaki M, Doebley JF, et al. A unified mixed-model method for association mapping that accounts for multiple levels of relatedness. Nat Genet. 2006;38(2):203–8.

122. Rincent R, Moreau L, Monod H, Kuhn E, Melchinger AE, Malvar RA, et al. Recovering power in association mapping panels with variable levels of linkage disequilibrium. Genetics. 2014;197(1):375–87.

123. Bradburd GS, Ralph PL, Coop GM. Disentangling the effects of geographic and ecological isolation on genetic differentiation. Evolution. 2013;67(11):3258–73.

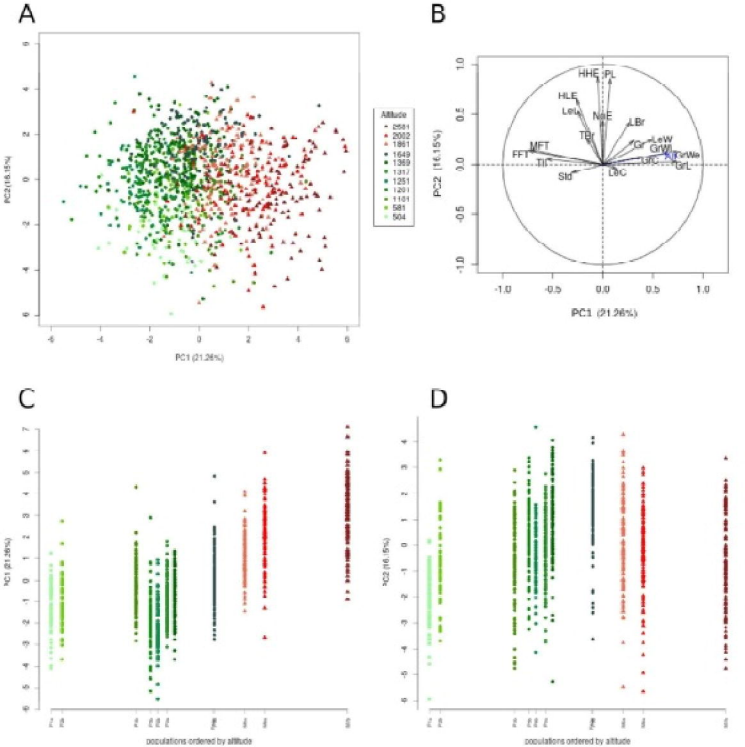
A
B
C
D
PC1 (21.26%)
PC2 (16.15%)
Altitude
2581
2002
1861
1649
1369
1317
1251
1201
1161
581
504
HHE
PL
HLE
LeL
NoE
LBr
TBr
LeW
GrW
GrWe
GrL
MFT
FFT
TIT
Std
LeC
populations ordered by altitude

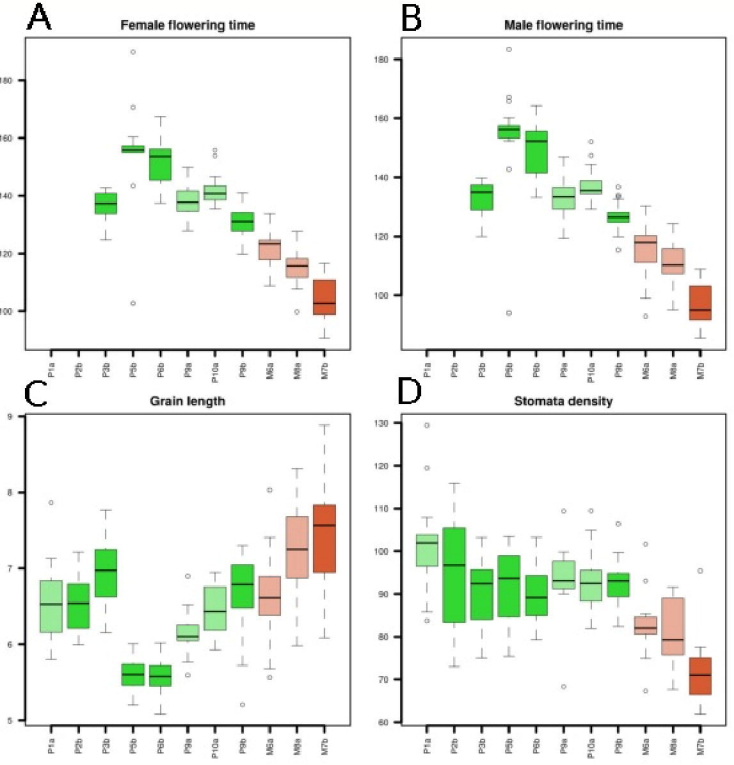
A
Female flowering time
B
Male flowering time
C
Grain length
D
Stomata density
P1a
P2b
P3b
P5b
P6b
P9a
P10a
P9b
M5a
M8a
M7b

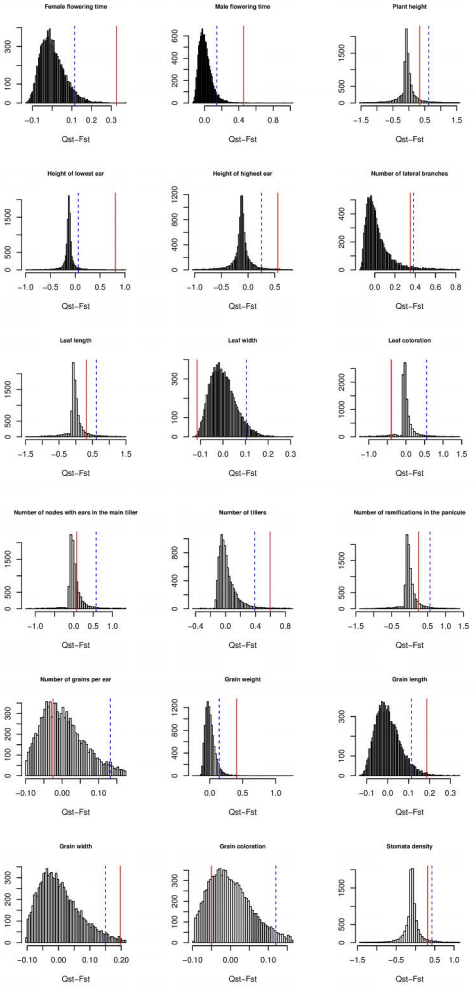
Female flowering time
Male flowering time
Plant height
Height of lowest ear
Height of highest ear
Number of lateral branches
Leaf length
Leaf width
Leaf coloration
Number of nodes with ears in the main tiller
Number of tillers
Number of ramifications in the panicule
Number of grains per ear
Grain weight
Grain length
Grain width
Grain coloration
Stomata density
Qst−Fst

A.

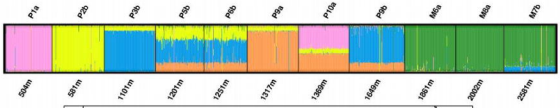
P1a
P2b
P3b
P5b
P6b
P9a
P10a
P9b
M6a
M8a
M7b
504m
951m
1101m
1201m
1251m
1317m
1369m
1640m
1961m
2002m
2591m

B.

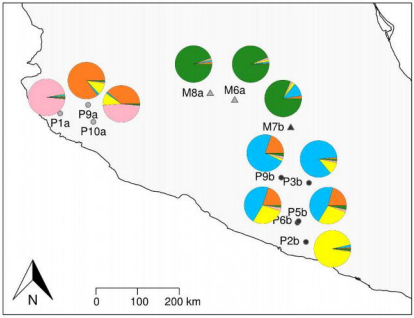
M8a
M6a
M7b
P9a
P10a
P1a
P9b
P3b
P5b
P6b
P2b
N
0
100
200 km

C.

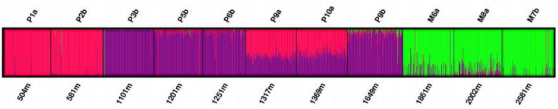
P1a
P2b
P3b
P5b
P6b
P9a
P10a
P9b
M6a
M8a
M7b
504m
951m
1101m
1201m
1251m
1317m
1369m
1640m
1961m
2002m
2591m

D.

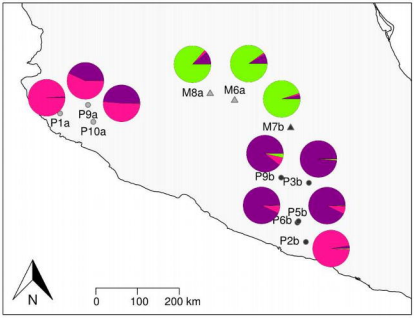
M8a
M6a
M7b
P9a
P10a
P1a
P9b
P3b
P5b
P6b
P2b
N
0
100
200 km

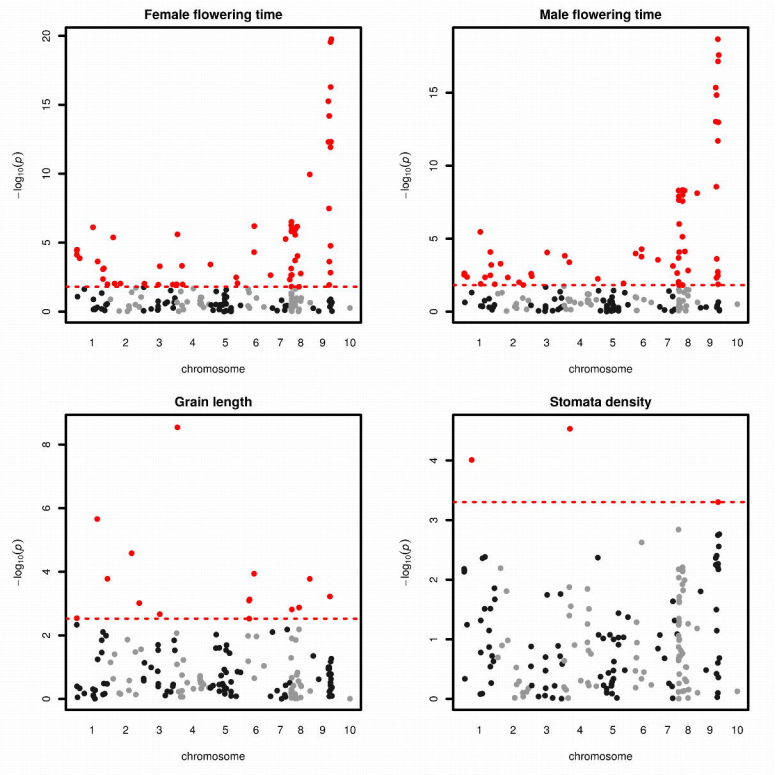
Female flowering time
Male flowering time
Grain length
Stomata density
$-\log_{10}(p)$
chromosome
1 2 3 4 5 6 7 8 9 10

A

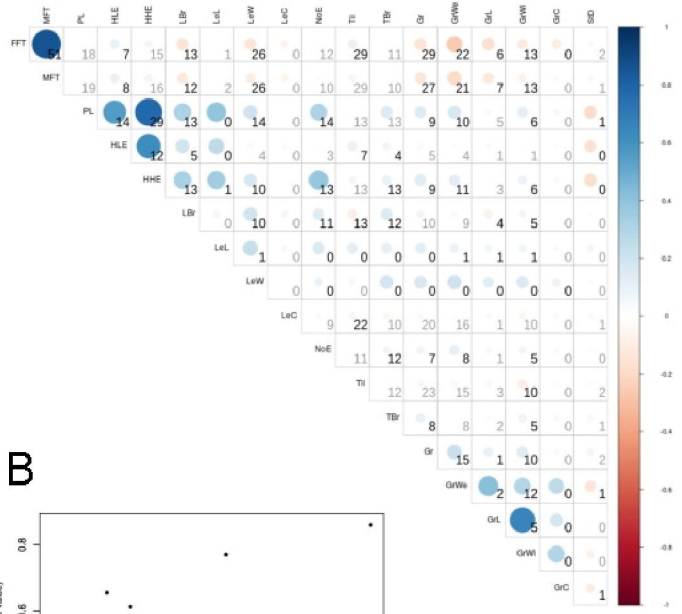
MFT
PL
HLE
HHE
LBr
LeL
LeW
LeC
NoE
Til
TBr
Gr
GrWe
GrL
GrWi
GrC
SiD
FFT
1
0.8
0.6
0.4
0.2
0
-0.2
-0.4
-0.6
-0.8
-1

B

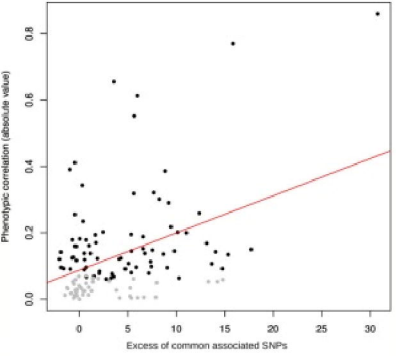
Phenotypic correlation (absolute value)
Excess of common associated SNPs
0.0
0.2
0.4
0.6
0.8
0
5
10
15
20
25
30